

Calvarial suture interdigitation in hadrosaurids (Ornithischia: Ornithopoda): Perspectives through ontogeny and evolution

Thomas W. Dudgeon^{1,2}  | David C. Evans^{1,2}

¹Department of Ecology and Evolutionary Biology, University of Toronto, Toronto, Ontario, Canada

²Department of Natural History, Royal Ontario Museum, Toronto, Ontario, Canada

Correspondence

Thomas W. Dudgeon, Department of Ecology and Evolutionary Biology, University of Toronto, Toronto, ON M5S 1A1, Canada.
Email: thomas.dudgeon@mail.utoronto.ca

Funding information

Ontario Graduate Scholarship; NSERC Vanier Canada Graduate Scholarship; NSERC Discovery Grant; Dinosaur Research Institute

Abstract

Lambeosaurine hadrosaurids exhibited extreme modifications to the skull, where the premaxillae, nasals, and prefrontals were modified to form their iconic supracranial crests. This morphology contrasts with their sister group, Hadrosaurinae, which possessed the plesiomorphic arrangement of bones. Although studies have discussed differences between lambeosaurine and hadrosaurine skull morphology and ontogeny, there is little information detailing suture modifications through ontogeny and evolution. Suture morphology is of particular interest due to its correlation with the mechanical loading of the skull in extant vertebrates. We quantify and contrast the morphology of calvarial sutures in iguanodontians and ontogenetic series of *Corythosaurus* and *Gryposaurus* to test whether the evolution of lambeosaurine crests impacted the mechanical loading of the skull. We found that suture interdigitation (SI) increases through ontogeny in hadrosaurids, although this increase is more extreme in *Corythosaurus* than *Gryposaurus*, and overall suture complexity (i.e., overall shape) remained constant. Lambeosaurines also have higher SI than other iguanodontians, even in crestless juveniles, suggesting that increased sinuosity is unrelated to the structural support of the crest. Hadrosaurines and basal iguanodontians did not differ. Similarly, lambeosaurines have more complexly shaped sutures than hadrosaurines and basal iguanodontians, while the latter two groups do not differ. Taken together, these results suggest that lambeosaurine calvarial sutures are more interdigitated than other iguanodontians, and although suture sinuosity increased through ontogeny, the suture shape remained constant. These ontogenetic and evolutionary patterns suggest that increased suture complexity in lambeosaurines coincided with crest evolution, and corresponding modifications to their facial skeleton altered the distribution of stress while feeding.

KEYWORDS

Hadrosauridae, morphometrics, suture interdigitation

This is an open access article under the terms of the Creative Commons Attribution License, which permits use, distribution and reproduction in any medium, provided the original work is properly cited.

© 2023 The Authors. *Evolution & Development* published by Wiley Periodicals LLC.

1 | INTRODUCTION

Suture morphology has become increasingly relevant in the last few decades for studying cranial biomechanics, with numerous studies focusing on suture morphology to infer mechanical loading (e.g., Gruntmejer et al., 2019; Kammerer, 2021; Markey & Marshall, 2007; Porro et al., 2015). Cranial sutures are unossified syndesmotomic joints that occur between the growth fronts of adjacent bones of the skull. Sutures have two main functions: (1) they are the primary regions of bone growth in the skull, and (2) they absorb mechanical stress by deforming, allowing the skull to respond to biomechanical loads. Suture growth and morphology are regulated by a complex set of biochemical and epigenetic factors (Herring, 1993; Jaslow, 1990). Due to their key role in cranial growth, suture patency in the calvarium (cranial vault) appears to be necessary in the early development of most vertebrates (Baer, 1954; Enlow, 1989; Jaslow, 1990; White et al., 2021). Sutures may close (i.e., fuse) once the period of rapid growth has ceased, but other factors such as biomechanical loading may result in the maintenance of patent (open) cranial sutures throughout the life span of an organism. This is because cranial suture morphology and patency are also influenced by mechanical stresses (Byron et al., 2018; Herring, 1993), and the biomechanical environment is an epigenetic factor thought to be the primary determinate of cranial suture morphology (Byron et al., 2018; Jaslow, 1990; Monteiro & Lessa, 2000; Moss, 1954, 1957, 1961; Rafferty & Herring, 1999). Sutures may remain simple, increase in their sinuosity, or close through ossification across the synarthroses through ontogeny depending on changes in the type and magnitude of load applied to the suture (Jaslow, 1990).

Cranial sutures have been repeatedly identified to exhibit distinct morphologies that are each best adapted to withstand specific types of mechanical loads (Herring & Mucci, 1991; Herring, 1972, 2008): lapping (scarf) joints are able to withstand highly variable loading regimes, including torsional forces; tongue-and-groove sutures are best able to withstand tension; similarly, butting sutures are able to handle tension; and finally, interdigitated sutures are best able to withstand compressive and tensional forces. These differences in suture mechanics are achieved due to the differing arrangement of the sutural ligament fibers, which absorb stress under tension and shear stress (Herring, 1972). For example, the interfingering of bones in an interdigitated suture allows the sutural ligament to be loaded with tension and shear forces along the interdigitations when the suture is under compression (Herring, 2008), but the increase in surface area works equally well when the suture is under

tension (Herring & Teng, 2000). The calvarium of vertebrates is therefore often composed of interdigitated sutures to better withstand the complex compressive and tensional forces exerted by the masticatory muscles attaching to the temporal region (e.g., Anderson & Bolt, 2013; Herring & Mucci, 1991; Herring & Teng, 2000; Herring, 1972; Kathe, 1999; Markey & Marshall, 2007). The degree of interdigitation in the calvarium has been directly correlated with the magnitude of mechanical stress exhibited by bite force (e.g., Byron et al., 2018), and calvarial suture interdigitation is therefore a helpful tool to evaluate mechanical loading in the skull. At present, the majority of detailed work on suture morphology and related mechanics has been carried out on mammals (e.g., Byron et al., 2018; Herring & Mucci, 1991; Herring & Teng, 2000; Herring, 1972, 1993; Jaslow, 1989, 1990; Savoldi et al., 2019), though there have been some detailed studies on reptiles (Monteiro & Lessa, 2000), and fish (Markey & Marshall, 2007).

Given the strong link between form and function in cranial sutures, many studies have used suture morphology to predict loading patterns in fossil taxa (e.g., Gruntmejer et al., 2019; Kammerer, 2021; Kathe, 1999), with subsequent finite element analyses demonstrating accuracy in predicting overall patterns of stress distribution (e.g., Fortuny et al., 2015; Maloul et al., 2014; Rayfield, 2005). However, few studies have used suture shape as a proxy for mechanical loading of the skull in dinosaurs (e.g., Rayfield, 2004, 2005; Weishampel, 1984), despite the diversity of cranial anatomy in the group (e.g., Brusatte et al., 2011; Felice et al., 2020; Foth et al., 2016). Potentially the most extreme modifications to the arrangement of the facial skeleton are observed in lambeosaurine hadrosaurs, where the premaxilla, nasals, and prefrontals were modified to form and support their supracranial crests. This morphology in lambeosaurines contrasts starkly with their sister group, Hadrosaurinae (=Saurolophinae), which possesses the plesiomorphic elongate skull condition and arrangement of bones. Although many studies have discussed anatomical differences between lambeosaurines and hadrosaurines, and changes through ontogeny (e.g., Brink et al., 2011; Evans, 2010; Evans et al., 2005; Prieto-Marquez, 2010; Weishampel, 1984), there is an absence of information detailing suture modification due to crest development. Discussing changes in suture morphology is significant since previous studies have suggested that lambeosaurines and hadrosaurines may have been specialized for processing different types of plants based on skull morphology, body proportions, and tooth wear (Carrano et al., 1999; Chapman & Brett-Surman, 1990; Dodson, 1975; Erickson et al., 2012; Mallon, 2019; Mallon & Anderson, 2013; Nabavizadeh, 2016). Additionally,

patterns of ontogenetic suture development are rarely documented in extinct vertebrates, and as such the paleobiological implications of their evolution are rarely explored. Although supracranial crests are absent in juvenile lambeosaurines and rapidly develop into maturity, juvenile lambeosaurines still exhibit rearrangement of the premaxilla, nasal, and prefrontal, suggesting differences in stress distribution may exist at birth.

Weishampel (1984) provided a detailed breakdown of cranial suture morphologies within Ornithopoda, but often treated Hadrosauridae with a single description, either not reporting on differences within the clade or attributing differences in suture morphology to support the weight of the lambeosaurine supracranial crest. However, changes in the distribution of mechanical stress throughout the skull while chewing is an alternate hypothesis that may pose a larger effect due to the extreme modifications to the bones of the snout in lambeosaurines. Here, we contrast the morphology of calvarial sutures between the lambeosaurine *Corythosaurus* and the contemporaneous hadrosaurine *Gryposaurus notabilis* through well-preserved ontogenetic series to test the following: (1) lambeosaurine calvarial suture interdigitation differed from other iguanodontians to support the weight of the supracranial crest; (2) lambeosaurine calvarial suture interdigitation differed from other iguanodontians due to differences in the distribution of stress through the skull during feeding. We then expand this comparison to include other lambeosaurines, hadrosaurines, and basal iguanodontians to provide a phylogenetic context for ontogenetic suture interdigitation patterns. Calvarial sutures were selected due to their close association with the masticatory muscles, and the well-documented relationship between calvarial suture complexity and mechanical stress.

2 | MATERIALS AND METHODS

2.1 | Materials

Images were taken of relevant specimens in dorsal view to capture the size and shape of the interfrontal and frontoparietal sutures, with a scale bar for reference (see Supporting Information: Table S1 for a list of specimens). Specimens that could not be evaluated in person were supplemented with dorsal braincase images from the literature (see Supporting Information: Table S1 for a list of specimens and their source). Although a two-dimensional view of the suture surface does not capture complete information on the three-dimensional suture face, isolated calvarial bones in iguanodontians show that

they are fairly consistent in suture interdigitation along these sutural contacts, and studying the suture surface is, therefore, a good approximation of suture shape. *Gryposaurus* specimens were identified as species following Lowi-Merri and Evans (2020) and Mallon et al. (2022). Isolated lambeosaurine braincases from Dinosaur Park were tentatively identified by us as *Lambeosaurus* if the frontal-nasal suture formed a raised ridge, and as *Corythosaurus* if this ridge was absent.

The following clade definitions are used when discussing phylogenetic positions of taxa in this study: Iguanodontia, all ornithopods more closely related to *Parasaurolophus walkeri* than to *Hypsilophodon foxii* or *Thescelosaurus neglectus* (Sereno, 2005); Hadrosauridae, the most recent common ancestor of *Sauroplophus osborni* and *P. walkeri* and all descendants (Sereno, 1998); Hadrosaurinae, all hadrosaurids more closely related to *S. osborni* than to *P. walkeri* (Sereno, 1998); Lambeosaurinae, all hadrosaurids more closely related to *P. walkeri* than to *S. osborni* (Sereno, 1998). We follow Xing et al. (2022) in using the term Hadrosaurinae over Sauroplophinae given that these clades are functionally the same except for the inclusion of *Hadrosaurus* in Hadrosaurinae.

Specimens were categorized into one of three ontogenetic age bins: juvenile, subadult, and adult. These bins were based on skull length, following Evans (2010): juvenile, less than 50% maximum skull length; subadult, 50%–85% maximum skull length; adult, above 85% maximum skull length. When complete skulls were not preserved, specimen size was estimated based on the size of preserved bones relative to other specimens. If only a small number of skulls were known for a taxon, making relative skull length inaccurate, ontogenetic age was assigned using the literature. It should be noted that this method of binning artificially partitions continuous growth and variation into discrete bins, but it is a useful metric for discussing ontogenetic skull growth in hadrosaurids because they represent the three distinct stages of crest development: juvenile, crest-less; subadult, rapid crest growth; adult, fully derived crests with little growth.

2.2 | Suture sinuosity

To quantify suture interdigitation, we employed the suture sinuosity index (SI), which is a measure of the sinuous length of a suture following the curves relative to its absolute length in a straight line from start to end (Supporting Information: Figure S1A,B; White et al., 2020). The closer the SI is to 1, the closer the suture is to a straight line, whereas higher SI values indicate

increased sinuosity. Images were loaded into ImageJ v1.53k (Schneider et al., 2012) and size calibrated using the “set scale” function. Suture lengths, defined as the sinuous length of the suture from end to end, were then measured for the interfrontal and the left and right frontoparietal sutures by tracing the sutures manually using the “lines” function set to “freehand.” Suture distances, defined as a straight line from one end of the suture to the other, were then measured using the “lines” function set to “straight.” The start of the interfrontal suture was defined as the posterior-most junction of the two frontal bones, and the end of the interfrontal suture was defined as the anterior-most ectocranial junction of the two frontals. For the frontoparietal suture, the suture started at the midline of the interfrontal process (the same start-point for the interfrontal suture) and ended at the lateral-most contact between the frontal and parietal. The suture SI was then calculated as the suture length divided by the suture distance, producing a unitless value to describe the sinuosity of the suture. Left and right frontoparietal suture SI values were averaged for subsequent analyses.

We subjected the interfrontal and average frontoparietal SI for *Corythosaurus* and *G. notabilis* to an analysis of covariance (ANCOVA) to evaluate whether there were significant differences in sinuosity between these taxa when ontogeny is considered as a covariate. This was done in RStudio v1.4.1106 using the “aov” and “Anova” functions from the package *stats* v4.0.4 (R Core Team, 2021), with “type” set to III. A second ANCOVA was then run on the full data set, comparing lambeosaurines to hadrosaurines and basal iguanodontians, with ontogeny as a covariate.

To visualize these data, we plotted the log-transformed suture lengths against their corresponding suture distances to visualize potential allometric differences between *Corythosaurus* and *Gryposaurus*. We then constructed two sets of boxplots using the “boxplot” function from the package *graphics* v4.0.4 (R Core Team, 2021). The first set was the SI for *Corythosaurus* and *Gryposaurus* at each ontogenetic stage. The second set was the SI for all specimens of lambeosaurines, hadrosaurines, and basal iguanodontians, binned according to their genus and ontogenetic stage (see Supporting Information: Table S1 for specimens and identifications).

2.3 | Suture complexity

To evaluate suture complexity (i.e., the shape of the suture), we implemented a windowed short-time Fourier transformation (STFT) with a power spectrum density (PSD) estimate. Fourier analyses compare contours by

generating coefficients defining the sine/cosine waves that together form the original curve (Allen, 2006). PSD estimates use the STFT coefficients to describe how the variance (i.e., power) is distributed within frequency intervals of the curve (Stoica & Moses, 1997), and is therefore used to indicate patterns among waves and curves (Allen, 2006). STFT with PSD has been used to describe suture complexity in invertebrates (Supporting Information: Figure S1C,D; Allen, 2006), but recent comparative studies have demonstrated their utility and accuracy in vertebrate suture complexity (White et al., 2020). PSD is useful in addition to SI because it quantifies the differences in suture shape that SI does not detect. Although White et al. (2020) used the total PSD to compare suture shape, we have chosen to bin the harmonics according to Allen (2006) to better illustrate potential differences between taxa.

Suture curves were digitized in R (R Core Team, 2021) using the “digitizeImages” function in the StereoMorph package (Olsen & Westneat, 2014). A single curve was drawn for each suture in the digitizeImages window, starting at the junction between the left and right frontoparietal sutures and the interfrontal suture, and ending at the lateral-/anterior-most extent of the sutures. Sutures were scaled using the scaling feature in the digitizeImages window. Suture curves were then re-sampled using the “readland.Shapes” function in the geomorph package (Adams et al., 2021; Baken et al., 2021) to produce 500 evenly spaced landmarks along each suture. The landmarks for each suture were separately scaled and aligned using a general Procrustes alignment (GPA) through the geomorph function “gpa-gen,” with the start and end landmarks set as fixed landmarks, and the remaining 498 landmarks set as sliding semilandmarks that were allowed to slide along their tangent plane.

Aligned and scaled coordinates were subjected to STFT using the function “stft” from the e1071 package (Meyer et al., 2021). The PSD was then calculated for each frequency as the sum of the squared STFT coefficients. PSD values were then summed in bins to describe the variance of very-low- (VLF), low- (LF), medium- (MF), and high-frequency (HF) waves in the sutures. These bins were defined following Allen (2006): VLF, 1–4 (broad and shallow lobes); LF, 5–12 (narrow lobes); MF, 12–32 (highly multilobate sutures); HF, 32< (serrations and other HF subdivisions). Although previous studies have focused on the total PSD value for a suture (i.e., PSD summed across all frequencies, without binning), we instead chose to bin the PSD frequencies to better illustrate differences in extremes (Allen, 2006). Lastly, we determined the proportion of each bin by dividing the bin power value by the total power for the

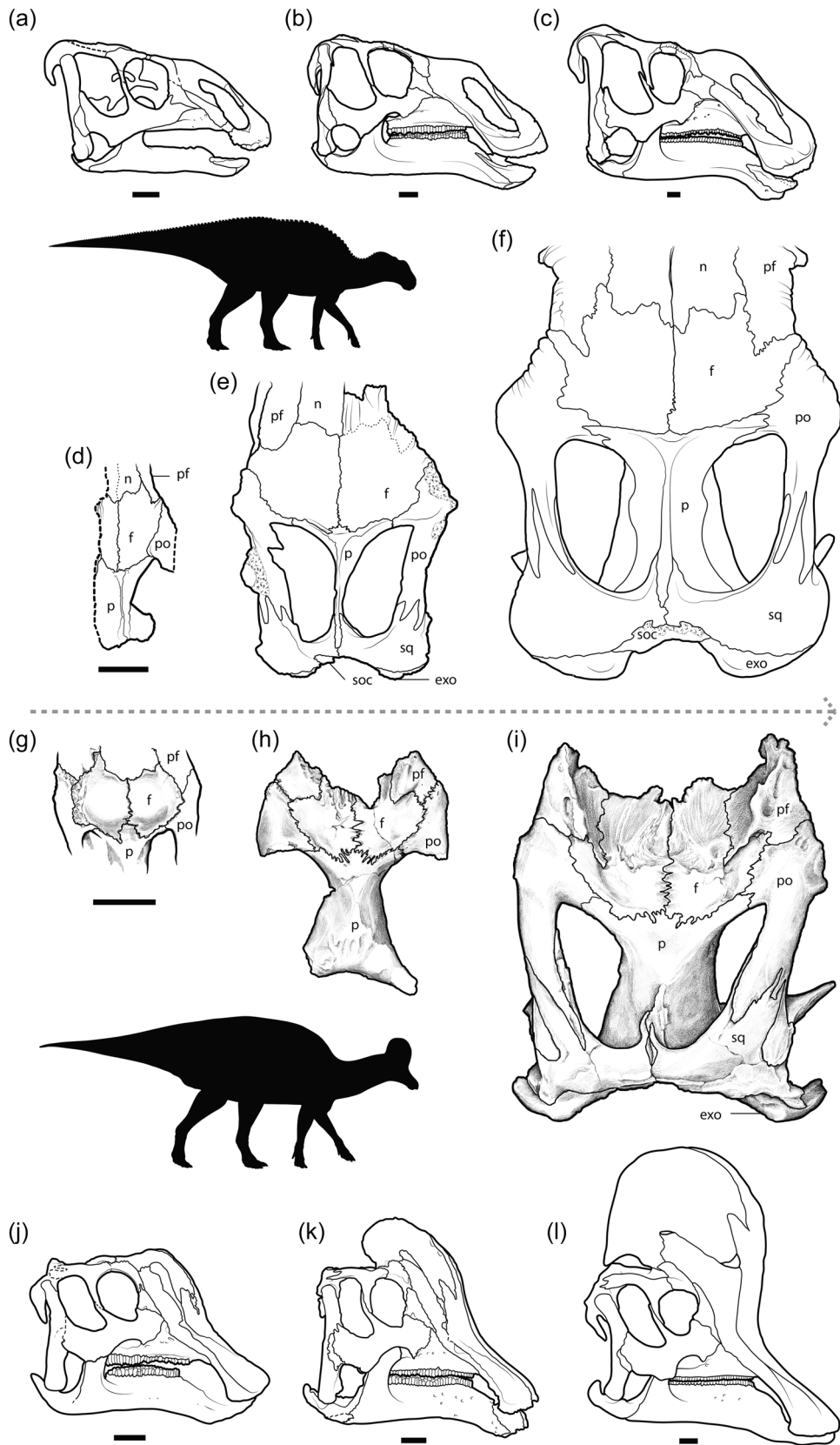


FIGURE 1 (See caption on next page)

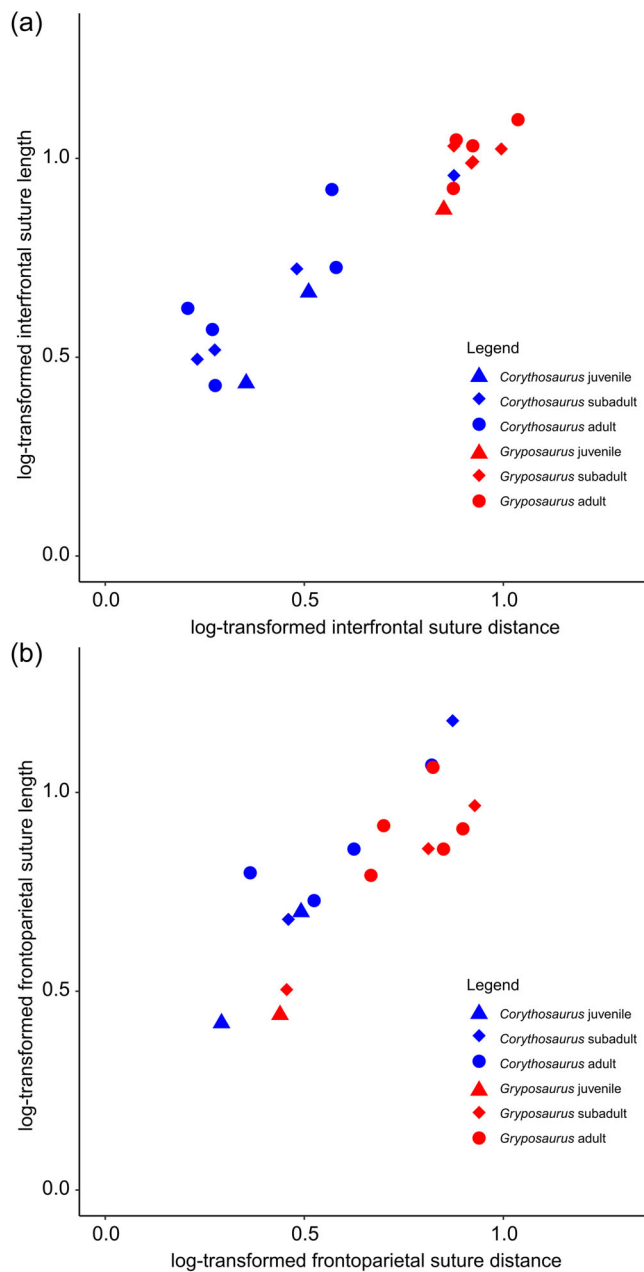


FIGURE 2 Log-transformed interfrontal suture length versus suture distance (a), and log-transformed right frontoparietal suture length versus suture distance (b). The right frontoparietal suture was chosen for plotting due to the larger sample size. [Color figure can be viewed at wileyonlinelibrary.com]

suture and multiplying by 100, allowing suture complexity to be compared between individuals.

We subjected the interfrontal and average frontoparietal PSD percentages of each suture for *Corythosaurus* and *G. notabilis* to an ANCOVA to evaluate whether there were significant differences in suture complexity between these taxa when ontogeny is considered as a covariate. This was done in RStudio v1.4.1106 using the “aov” and “Anova” functions from the package *stats* v4.0.4 (R Core Team, 2021), with “type” set to III. A second ANCOVA was then run on the full data set, comparing lambeosaurines to hadrosaurines and basal iguanodontians, with ontogeny as a covariate.

Finally, we constructed two sets of bar graphs using the “barplot” function from the package *graphics* v4.0.4 (R Core Team, 2021) to visualize suture complexity. The first set was the PSD bin percentages for *Corythosaurus* and *Gryposaurus* at each ontogenetic stage. The second set was the PSD bin percentages for all specimens of lambeosaurines, hadrosaurines, and basal iguanodontians, binned according to their genus and ontogenetic stage.

3 | RESULTS

3.1 | Suture sinuosity

Suture sinuosity clearly increases through ontogeny in both *Corythosaurus* and *Gryposaurus* (Figures 1, 2, and 3), supporting previous observations by Weishampel (1984). The juvenile *Gryposaurus* has the lowest observed SI among all specimens examined here, nearly equaling 1. The mature *Gryposaurus* have more sinuous sutures than their juvenile conspecifics, averaging approximately 1.2 for the interfrontal suture (1.12–1.46) and approximately 1.4 for the frontoparietal sutures (1.02–1.61). The lambeosaurine *Corythosaurus* has markedly higher SI across all ontogenetic stages. Juvenile *Corythosaurus* have an average interfrontal SI of approximately 1.3 (1.20–1.42), and a frontoparietal SI of approximately 1.6 (1.37–1.78). Subadult *Corythosaurus* have much higher SI values, averaging approximately 1.75 for the interfrontal

FIGURE 1 Ontogenetic series of *Gryposaurus notabilis* skulls in lateral view (a–c) and braincase roofs in dorsal view (d–f), and *Corythosaurus casuarius* braincase roofs in dorsal view (g–i) and skulls in lateral view (j–l). (a, d) Juvenile (Canadian Museum of Nature [CMN] 8784), (b, e) subadult (Royal Tyrrell Museum of Palaeontology [TMP] 1980.022.0001), (c, f) adult (Royal Ontario Museum [ROM] 873, c; AMNH 5350, f), (g, j) juvenile (ROM 759), (h, k) subadult (ROM 694, h; CMN 34825, k), (i, l) adult (ROM 1940, i; ROM 871, l). Corresponding body silhouettes represent *G. notabilis* and *C. casuarius*. Arrow indicates ontogenetic trajectory. Scale bars represent 5 cm. exo, exoccipital; f, frontal; n, nasal; p, parietal; pf, prefrontal; po, postorbital; soc, supraoccipital; sq, squamosal. Line art by D. Dufault and K. Dupuis, silhouettes by D. Dufault.

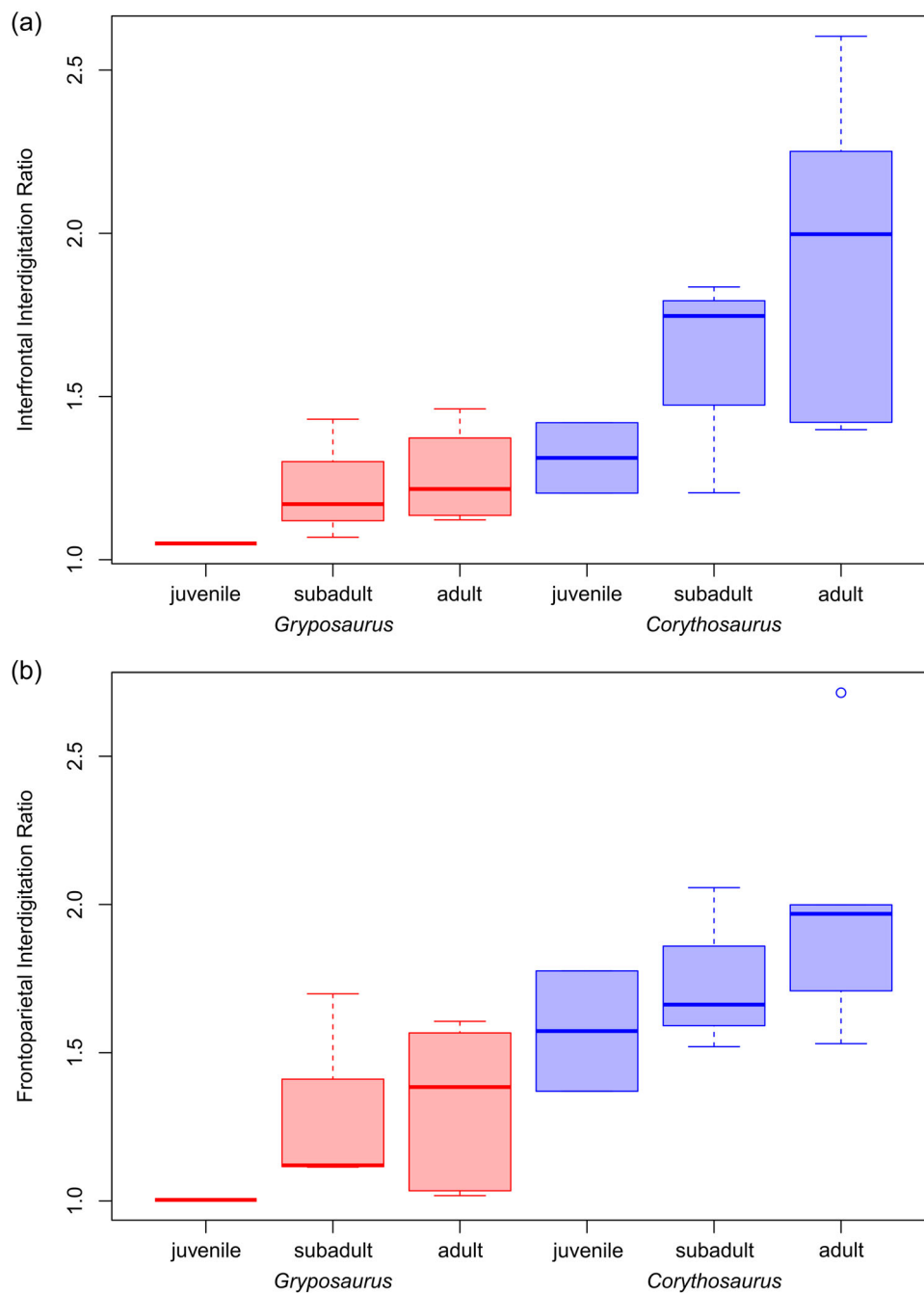


FIGURE 3 Sinuosity index for (a) the interfrontal suture, and (b) the average frontoparietal suture for juvenile, subadult, and adult *Corythosaurus* and *Gryposaurus*. Thick bars represent the mean, boxes represent the upper and lower quartiles, and whiskers represent the maximum and minimum values. [Color figure can be viewed at wileyonlinelibrary.com]

(1.20–1.83) and 1.8 for the frontoparietal (1.52–2.06) sutures. Mature *Corythosaurus* had the highest SI among these two genera, averaging approximately 1.7 for the interfrontal suture (1.40–2.60) and 1.9 for the frontoparietal suture (1.53–2.71). The interfrontal suture is much shorter on average in all ontogenetic stages of *Corythosaurus* than *Gryposaurus* (Figure 2), likely due to the shorter frontal platform in lambeosaurines. The frontoparietal suture, however, is similar in size between

Corythosaurus and *Gryposaurus*, but with higher interdigitation in the former taxon (Figures 2 and 3). Overall, SI tends to be similar between the frontoparietal and interfrontal sutures of *Gryposaurus*, but the frontoparietal sutures tend to be more sinuous than the interfrontal suture in *Corythosaurus*. This is an interesting observation, given that most *Gryposaurus* specimens observed here, in addition to specimens described by Weishampel (1984), tend to have interfrontal sinuosity

TABLE 1 ANCOVA of calvarial suture sinuosity index between *Corythosaurus* and *Gryposaurus*.

Suture	Variable	p Value
Interfrontal	Genus	0.002517
	Ontogenetic age	0.116506
Frontoparietal (average)	Genus	0.0009734
	Ontogenetic age	0.2401278

Note: Bold indicates statistical significance ($\alpha = 0.05$).

Abbreviation: ANCOVA, analysis of covariance.

concentrated in the posterior half of the suture (i.e., the posterior half of the interfrontal suture is more interdigitated than the anterior half). These observations suggest that increased sinuosity is common in the posterior calvarium of hadrosaurines and may reflect increased loading of forces in the posterior portion of the braincase, similar to the observations of Byron et al. (2018) in mice.

The ANCOVA found significant differences in both interfrontal and frontoparietal sinuosity between *Corythosaurus* and *Gryposaurus*, but did not find significant differences between ontogenetic ages (Table 1). Visually assessing sinuosity in the ontogenetic stages reveals that *Corythosaurus* is more sinuous than *Gryposaurus* at each stage, including the juvenile stage, and the only groups with similar sinuosity are juvenile *Corythosaurus* and mature *Gryposaurus*.

The trends observed between *Corythosaurus* and *Gryposaurus* are also true more broadly in Iguanodontia, where lambeosaurines consistently have more sinuous calvarial sutures than hadrosaurines (Figure 4). ANCOVA found significant differences in both interfrontal and frontoparietal SI (Table 2), and a post hoc Tukey's test found that this difference is significant between Lambeosaurinae and Hadrosaurinae, and Lambeosaurinae and basal Iguanodontia (Supporting Information: Table S2). No significant differences were found between Hadrosaurinae and basal Iguanodontia. Suture sinuosity also showed no significant differences between ontogenetic groups. Interestingly, the most extreme SI observed here was for the frontoparietal suture of the juvenile *Parasaurolophus* sp. (CMN 8502; Evans et al., 2007), a notable observation given that juveniles usually have lower sinuosity than mature individuals.

3.2 | Suture complexity

Differences in suture complexity as indicated by PSD bins are much more subtle, and ontogenetic trends are not clear for either genus (Figure 5). Interestingly, interfrontal PSD values differ little between *Corythosaurus* and

Gryposaurus, with significant differences present only in LF and HF features (Table 3). Frontoparietal PSD values are overall quite different between these two genera, where *Corythosaurus* has significantly more MF and HF features, and *Gryposaurus* has significantly more VLF features. There are no significant differences between these genera in LF features. No significant differences were found between ontogenetic age groups in either suture.

ANCOVA of PSD bins between Lambeosaurinae, Hadrosaurinae, and basal Iguanodontia reveals similar trends across this larger data set (Figure 6). Significant differences in the interfrontal suture occur in VLF, MF, and HF features, where lambeosaurines have significantly less VLF features than basal iguanodontians, more MF features than basal iguanodontians, and more HF features than hadrosaurines and basal iguanodontians (Table 4). We also found significant differences in the LF features across ontogenetic ages, though post hoc Tukey's test found no significant differences between groups (subadult–adult approach significance). Significant differences also occur in the frontoparietal sutures in VLF, MF, and HF features. Post hoc Tukey's tests indicate that all significant differences between phylogenetic groups are between Lambeosaurinae and Hadrosaurinae, and Lambeosaurinae and basal Iguanodontia, where Lambeosaurinae has more MF and HF features, and less VLF features, than Hadrosaurinae and basal Iguanodontia (Supporting Information: Table S3). The ANCOVA also recovered significant differences in VLF, MF, and HF features between ontogenetic stages in the frontoparietal suture, and post hoc Tukey's test reveals that these differences are only significant between the juvenile and adult groups (Supporting Information: Table S3).

4 | DISCUSSION

We found that the SI of *Corythosaurus* was significantly higher than *Gryposaurus*, a trend that was also true for lambeosaurines and hadrosaurines more broadly, supporting the hypothesis that suture sinuosity differs between lambeosaurines and hadrosaurines. Both taxa demonstrate an increase in sinuosity through ontogeny, an expected phenomenon given that bite force and jaw lever advantage increase with body size in hadrosaurids (Mallon & Anderson, 2015), along with suture sinuosity in ornithopods more generally (Weishampel, 1984). Sinuosity appears to be an ontogenetically rapid phenomenon in *Corythosaurus*, where sutures are simple or slightly sinuous in juvenile individuals, and dramatically increase in sinuosity leading into maturity, particularly for the

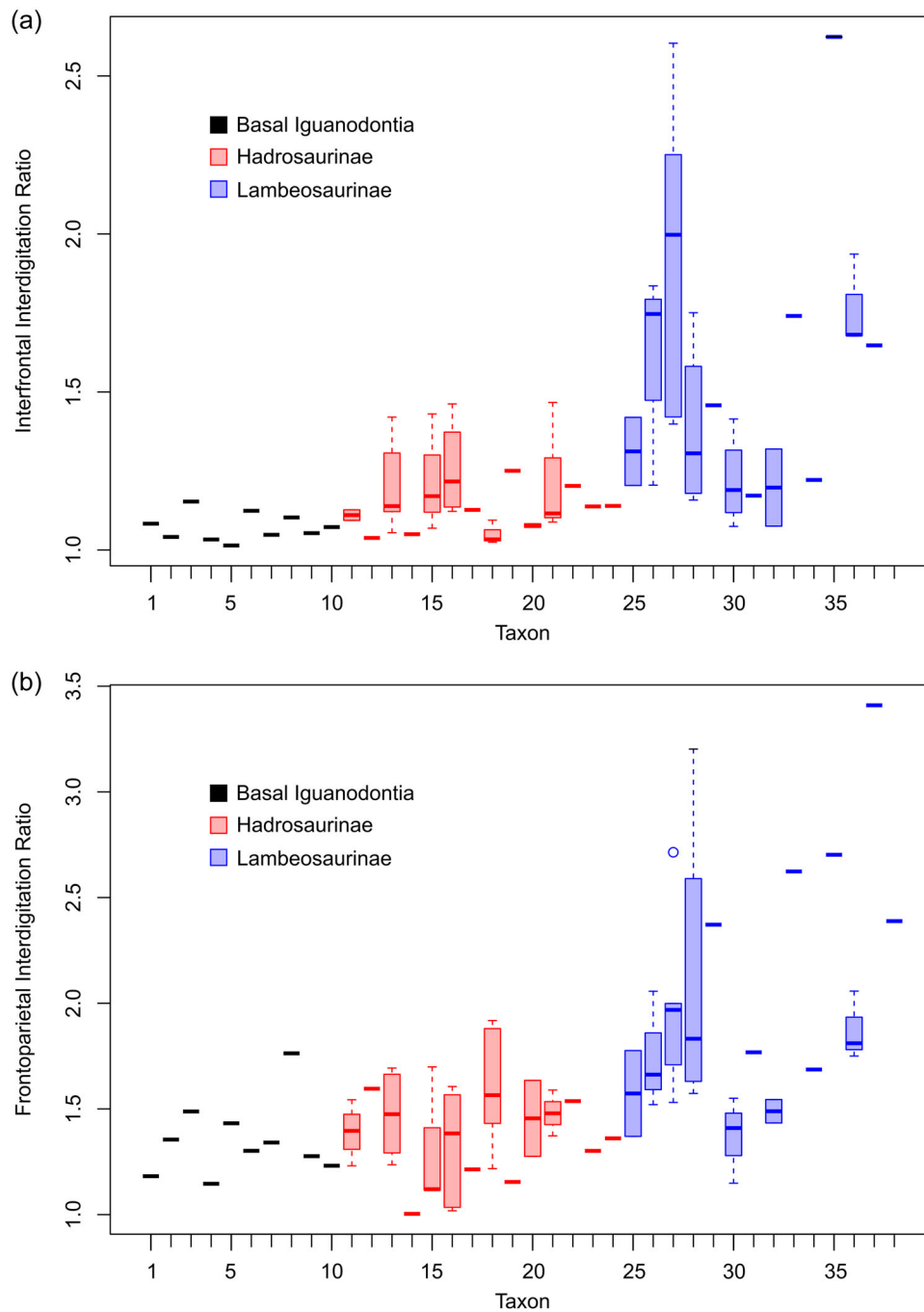


FIGURE 4 Sinuosity index for (a) the interfrontal suture, and (b) the average frontoparietal suture for lambeosaurines (blue, left), hadrosaurines (red, center), and basal iguanodontians (light blue, right). Thick bars represent the mean, boxes represent the upper and lower quartiles, and whiskers represent the maximum and minimum values. Taxon labels: 1, *Bactrosaurus* adult; 2, *Dysalotosaurus* juvenile; 3, *Eotrachodon* subadult; 4, *Gobihadros* adult; 5, *Jintasaurus* adult; 6, *Levnesovia* adult; 7, *Lophorhodon* juvenile; 8, *Sirindhorna* adult; 9, *Tanius* adult; 10, *Tenontosaurus* subadult; 11, *Edmontosaurus* juvenile; 12, *Edmontosaurus* subadult; 13, *Edmontosaurus* adult; 14, *Gryposaurus* juvenile; 15, *Gryposaurus* subadult; 16, *Gryposaurus* adult; 17, Hadrosaurinae subadult; 18, Hadrosaurinae adult; 19, *Maiasaura* adult; 20, *Prosaurolophus* juvenile; 21, *Prosaurolophus* subadult; 22, *Prosaurolophus* adult; 23, *Saurolophus* subadult; 24, *Shantungosaurus* adult; 25, *Corythosaurus* juvenile; 26, *Corythosaurus* subadult; 27, *Corythosaurus* adult; 28, *Hypacrosaurus* juvenile; 29, *Hypacrosaurus* subadult; 30, *Hypacrosaurus* adult; 31, *Jaxartosaurus* adult; 32, *Lambeosaurus* juvenile; 33, *Lambeosaurus* subadult; 34, *Lambeosaurus* adult; 35, Lambeosaurinae subadult; 36, Lambeosaurinae adult; 37, *Parasaurolophus* juvenile; 38, *Parasaurolophus* subadult. [Color figure can be viewed at wileyonlinelibrary.com]

interfrontal suture. Interestingly, skull size continues to increase after sinuosity has increased in subadults, and the degree of sinuosity does not change dramatically over the large size range from subadult to adult, the time when crests are rapidly growing. Although ontogenetic sinuosity of the calvarial bones does

occur in *Gryposaurus*, it is not comparable to the change in depth of sinuosity observed in *Corythosaurus* (Figure 3). The interfrontal suture, which is highly sinuous in subadult and larger lambeosaurines, is virtually straight in the dorsal view in most hadrosaurine and basal iguanodontian taxa.

PSD values also differ significantly between *Corythosaurus* and *Gryposaurus* calvarial sutures, though the interfrontal suture only showed differences in HF features. The frontoparietal suture showed notable differences between groups, suggesting a more dramatic difference in suture complexity between these taxa than the interfrontal. Comparisons between taxonomic groups within Iguanodontia show a similar trend, where the complexity of the interfrontal suture differs little between lambeosaurines, hadrosaurines, and basal iguanodontians (though lambeosaurines have more HF features than the latter two groups), and the frontoparietal suture

TABLE 2 ANCOVA of calvarial suture sinuosity index between Lambeosaurinae, Hadrosaurinae, and basal iguanodontia.

Suture	Variable	<i>p</i> Value
Interfrontal	Genus	7.802×10^{-8}
	Ontogenetic age	0.05792
Frontoparietal (average)	Genus	2.622×10^{-7}
	Ontogenetic age	0.1816

Note: Bold indicates statistical significance ($\alpha = 0.05$).

Abbreviation: ANCOVA, analysis of covariance.

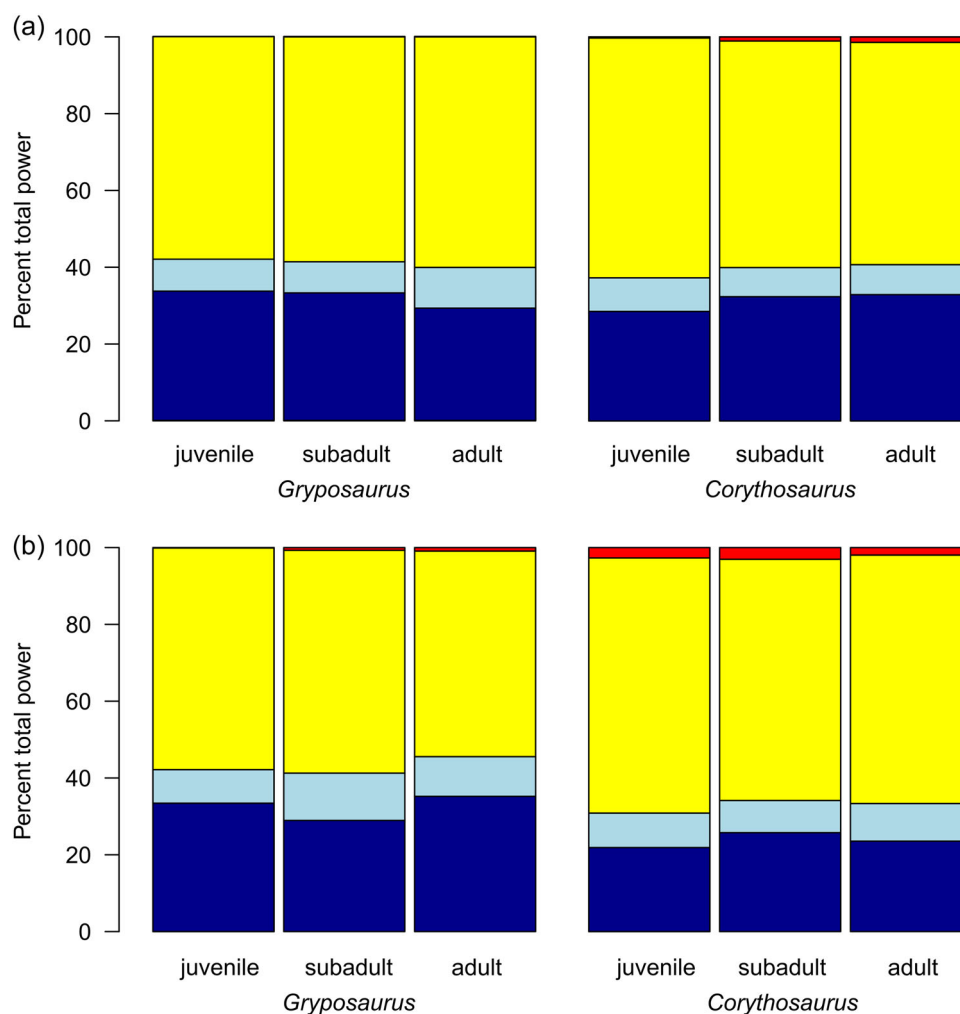


FIGURE 5 Proportion of total power for very low-frequency (dark blue), low-frequency (light blue), middle-frequency (yellow), and high-frequency (red) features for (a) the interfrontal suture, and (b) the average frontoparietal suture for the three ontogenetic ages of *Corythosaurus casuarius* and *Gryposaurus* sp. [Color figure can be viewed at wileyonlinelibrary.com]

TABLE 3 ANCOVA of calvarial suture PSD bins between *Corythosaurus* and *Gryposaurus*, and between ontogenetic ages.

Suture	Frequency bin	Variable	p Value
Interfrontal	VLF	Genus	0.5046
		Ontogenetic age	0.3567
	LF	Genus	0.03268
		Ontogenetic age	0.23576
	MF	Genus	0.7630
		Ontogenetic age	0.4259
	HF	Genus	0.0055
		Ontogenetic age	0.3226
Frontoparietal (average)	VLF	Genus	0.0006217
		Ontogenetic age	0.5060140
	LF	Genus	0.2504
		Ontogenetic age	0.6967
	MF	Genus	0.0002811
		Ontogenetic age	0.4716754
	HF	Genus	0.008816
		Ontogenetic age	0.852008

Note: Bold indicates statistical significance ($\alpha = 0.05$).

Abbreviations: ANCOVA, analysis of covariance; HF, high frequency; LF, low frequency; MF, middle frequency; PSD, power spectrum density; VLF, very low frequency.

is more complex in lambeosaurines than hadrosaurines and basal iguanodontians.

Taken together, the SI and PSD results suggest that although the interfrontal suture was more sinuous in lambeosaurines than in other iguanodontians, the complexity or overall shape of the suture differed little. This is contrasted with the frontoparietal suture, which was both more sinuous and more complex in lambeosaurines, meaning lambeosaurines have more lobes and serrations (i.e., HF features) in the suture than other iguanodontians. The combination of differences in sinuosity and complexity through phylogeny and ontogeny in Iguanodontia suggests that the increased sinuosity observed in lambeosaurines is associated with supracranial crest modifications to the skull. This suggests that the rearrangement of the cranial bones associated with the development of these crests forced significant changes in the physical loading of the skull, resulting in changes in suture morphology (Figure 7).

The similar pattern of suture sinuosity and complexity in the calvaria of lambeosaurines and hadrosaurines (i.e., increased sinuosity and complexity posteriorly) suggests that the skull roof of these groups likely experienced a similar pattern of loading when chewing, but the forces were more intense in lambeosaurines than hadrosaurines. It is well known that lambeosaurines

have smaller adult skull sizes than hadrosaurines (Mallon & Anderson, 2013), suggesting that lambeosaurines would have lower bite forces given that jaw lever advantage is isometric in hadrosaurids (Mallon & Anderson, 2015). It is therefore unlikely that the increased sinuosity observed in lambeosaurines is due to high bite forces, and instead suggests that mechanical stress was more concentrated in the calvaria of lambeosaurines compared to hadrosaurines and basal iguanodontians. Additionally, there is little evidence for broad dietary differences between lambeosaurines and hadrosaurines; lambeosaurines likely preferred low browse, and hadrosaurines likely preferred high browse, with significant niche overlap between these groups (Carrano et al., 1999; Mallon, 2017). It is, therefore, unlikely that the large differences in the calvarial suture pattern observed here are due to dietary differences. Weishampel (1984) suggested that differences in suture morphology between lambeosaurines and hadrosaurines may be due to the imparted strain on the calvarium from the large supracranial crests, but associated changes in the mechanical performance of the skull while chewing may have a greater influence due to the extreme modifications to the bones of the snout in lambeosaurines. The results presented here support the hypothesis that suture interdigitation is associated with feeding

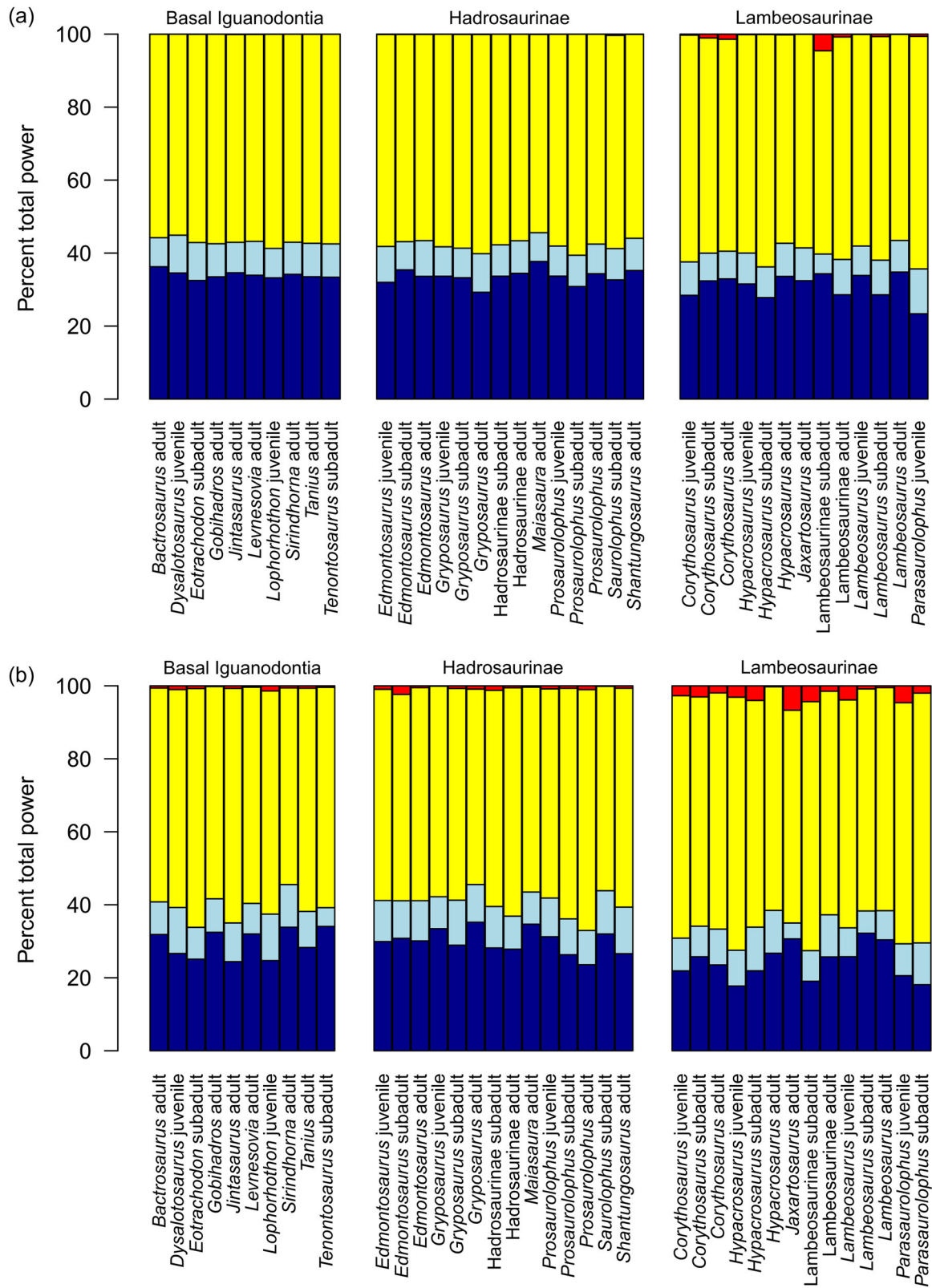


FIGURE 6 Proportion of total power for very-low-frequency (dark blue), low-frequency (light blue), middle-frequency (yellow), and high-frequency (red) features for (a) the interfrontal suture, and (b) the average frontoparietal suture for basal Iguanodontia (left), Hadrosaurinae (center), and Lambeosaurinae (right). [Color figure can be viewed at wileyonlinelibrary.com]

TABLE 4 ANCOVA of calvarial suture PSD bins between Lambeosaurinae, Hadrosaurinae, and basal Iguanodontia.

Suture	Frequency bin	Variable	p Value
Interfrontal	VLF	Group	0.04854
		Ontogenetic age	0.60049
	LF	Group	0.17974
		Ontogenetic age	0.04776
	MF	Group	0.0234
		Ontogenetic age	0.1515
	HF	Group	0.0001746
		Ontogenetic age	0.0707001
Frontoparietal (average)	VLF	Group	1.957 × 10⁻⁶
		Ontogenetic age	0.02038
	LF	Group	0.0772
		Ontogenetic age	0.9492
	MF	Group	7.471 × 10⁻⁸
		Ontogenetic age	0.02356
	HF	Group	4.261 × 10⁻⁷
		Ontogenetic age	0.02291

Note: Bold indicates statistical significance ($\alpha = 0.05$).

Abbreviations: HF, high frequency; LF, low frequency; MF, middle frequency; PSD, power spectrum density; VLF, very low frequency.

mechanics and not crest support, given that the juvenile lambeosaurines exhibit increased interdigitation above that of other iguanodontians before the crest has begun to develop. Although it is possible that the greater calvarial suture interdigitation in juvenile lambeosaurines is a genetically predisposed condition caused by the development of crests later in life, this is unlikely given the strong dependence of suture shape on mechanical loading of the skull through ontogeny in extant taxa (e.g., Byron et al., 2018; Herring, 1993). Interdigitation due to the structural support of the lambeosaurine supracranial crest also appears unlikely because these crests were formed by thin sheets of bone from the premaxillae and nasals that primarily housed air-filled expansions of the nasal passages and were therefore light. Additionally, the crested hadrosaurine *Saurolophus* does not exhibit increased interdigitation compared to other hadrosaurines and basal iguanodontians. This provides further evidence that increased suture interdigitation is not related to crest support, but instead the rearrangement of the facial skeleton in lambeosaurines to form the crest.

Jaslow's (1989, 1990) studies of sexual differences in suture morphology in wild sheep (*Ovis orientalis*) found that increased suture interdigitation in head-butting adult males was best correlated with horn size, providing an analogue for other supracranial structures.

Importantly, juveniles of both sexes, and mature female sheep, did not differ significantly in the level of suture interdigitation (Jaslow 1989), despite many female sheep possessing horns. These horns are largest in adult males, but most importantly, only males engage in head-to-head butting behavior. The increased interdigitation of cranial sutures in males is, therefore, an indication of the compensatory development of cranial sutures to cope with the added forces of head butting (Jaslow, 1989) and is not due to the presence and support of horns. This further suggests that increased interdigitation in lambeosaurines is not due to the support of supracranial structures, and instead suggests that they may be due to other mechanics affecting the skull. Lambeosaurine crests were obviously far too delicate to engage in physical confrontations like head butting (Hopson, 1975), indicating that increased stress during feeding is the likely mechanism for increased interdigitation in lambeosaurines.

The rearrangement of the facial skeleton in lambeosaurines also caused changes in the arrangement of cranial sutures, reflecting the distribution of mechanical stress. The expansion of the premaxilla onto and over the skull roof in lambeosaurines resulted in the snout being nearly devoid of sutures, save the premaxilla-maxilla suture, serving a stark contrast to the snout of

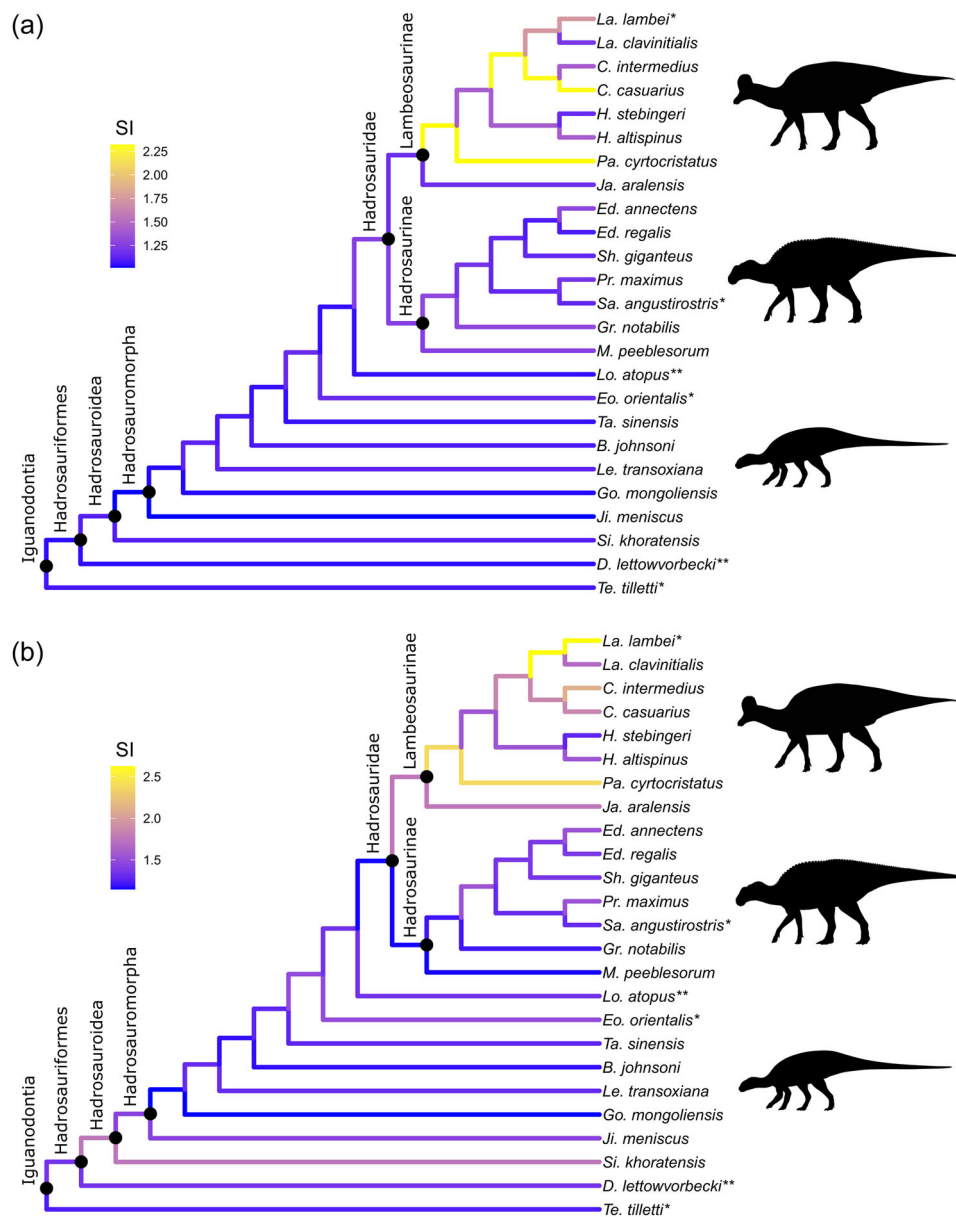


FIGURE 7 Suture interdigitation (SI) for the interfrontal (a) and frontoparietal (b) sutures mapped on a phylogeny of included taxa. Genus abbreviations: B., *Bactrosaurus*; C., *Corythosaurus*; D., *Dysalotosaurus*; Ed., *Edmontosaurus*; Eo., *Eotrachodon*; Go., *Gobihadros*; Gr., *Gryposaurus*; H., *Hypacrosaurus*; Ja., *Jaxartosaurus*; Ji., *Jintasaurus*; La., *Lambeosaurus*; Le., *Levnesovia*; Lo., *Lophorhodon*; M., *Maiasaura*; Pa., *Parasaurolophus*; Pr., *Parasaurolophus*; Sa., *Sauroplophus*; Sh., *Shantungosaurus*; Si., *Sirindhorna*; Ta., *Tanias*; Te., *Tenontosaurus*. * Taxa represented by subadults; ** indicates taxa represented by juveniles. Silhouettes by D. Dufault. [Color figure can be viewed at wileyonlinelibrary.com]

hadrosaurines that possess two premaxilla-nasal sutures and the premaxilla-maxilla suture. The absence of sutures in the snout of lambeosaurines suggests that mechanical stress is not dissipated (i.e., absorbed) efficiently in the snout, and may instead be transferred posterodorsally through the solid premaxilla. The transfer of stress posterodorsally could, therefore, result in greater loading of more posterior sutures, and may be an explanation for increased calvarial sutures in lambeosaurines. If true, this may also explain why the

premaxilla forms an ossified septum between the anterior nasal passages in lambeosaurines while the septum remains unossified in hadrosaurines. Additionally, lambeosaurines possess a tongue-and-groove lacrimal-maxilla suture, and an interdigitated lacrimal-prefrontal suture, both of which are more complex than the simple scarf joints in hadrosaurines (Weishampel, 1984). Lambeosaurines are further unique in having a contact between the prefrontal and postorbital, which is also interdigitated. This combination of complex sutures

posterior to the snout is consistent with the hypothesis that lambeosaurines experienced increased loading in this region. Greater posterior transfer of mechanical stress within the skull of lambeosaurines than hadrosaurines and basal iguanodontians would likely require the sutures in the posterior region of the skull to be better adapted to absorb this stress. These complex joints in lambeosaurines, combined with increased interdigitation of the calvarial sutures in these animals, suggest that lambeosaurines experienced significantly different loading regimes than other iguanodontians. Our work presented here provides new evidence that feeding mechanics differ between lambeosaurines and hadrosaurines due to the development of the prominent lambeosaurine supracranial crest. At present, feeding has only been completely digitally modeled in hadrosaurines (Bell et al., 2009; Rybczynski et al., 2008). In the future, we will test the stress distribution pattern outlined here across Hadrosauridae using finite element analysis.

AUTHOR CONTRIBUTIONS

Thomas W. Dudgeon and David C. Evans devised the project and determined methodology. Thomas W. Dudgeon collected the data, conducted the analyses, constructed the tables and figures, and wrote the manuscript. David C. Evans supervised the project and edited the manuscript.

ACKNOWLEDGMENTS

This research was conducted on Treaty 13 land, the traditional home of the Huron-Wendat, the Seneca, and the Mississaugas of the Credit. Specimens examined at the Royal Ontario Museum (ROM, Toronto, ON, Canada), Canadian Museum of Nature (CMN, Ottawa, ON, Canada), and Royal Tyrrell Museum of Palaeontology (TMP, Drumheller, AB, Canada) were found on the ancestral land of the Blackfoot Confederacy. Travel restrictions and museum closures caused by the COVID-19 pandemic heavily impacted data collection for this study, and we are grateful to the following people for their patience and kindness in providing photos and access to specimens for this study: Kevin Seymour, Brian Iwama, Ian Morrison, and Talia Lowi-Merri (ROM); Scott Rufolo, Margaret Currie, Shyong en Pan, and Jordan Mallon (CMN); Rhian Russell, Becky Sanchez, Tom Courtenay, and Brandon Strilisky (TMP); Kirsten Brink (MU); and Phil Bell (UNE). We also thank Zoe Landry for helpful discussions on our statistical approach, Aaron Olsen for advice with StereoMorph, Heather White for assistance with executing and interpreting PSD, Lindsay Zanno for constructive comments, and Robert Reisz for early support. The line art was

kindly made by Danielle Dufault and Kevin Dupuis, and the silhouettes were made by Danielle Dufault. The funding for this project was provided by a Dinosaur Research Institute grant, Ontario Graduate Scholarship, and NSERC Vanier Canada Graduate Scholarship to Thomas W. Dudgeon, and an NSERC Discovery Grant to David C. Evans (RGPIN-2018-06788).

CONFLICT OF INTEREST STATEMENT

The authors declare no conflict of interest.

DATA AVAILABILITY STATEMENT

The data that supports the findings of this study are available in the Supporting Information: Material of this article. The suture interdigitation ratios are provided in the Supporting Information.

ORCID

Thomas W. Dudgeon  <http://orcid.org/0000-0002-0976-8599>

REFERENCES

- Adams, D. C., Collyer, M. L., Kaliontzopoulou, A., & Baken, E. K. (2021). *Geomorph: Software for geometric morphometric analyses. R package version 4.0.2.* <https://cran.r-project.org/package=geomorph>.
- Allen, E. G. (2006). New approaches to Fourier analysis of ammonoid sutures and other complex, open curves. *Paleobiology*, 32(2), 299–315.
- Anderson, J. S., & Boltz, J. R. (2013). New information on amphibamids (Tetrapoda, Temnospondyli) from Richards Spur (Fort Sill), Oklahoma. *Journal of Vertebrate Paleontology*, 33(3), 553–567.
- Baer, M. J. (1954). Patterns of growth of the skull as revealed by vital staining. *Human Biology*, 26, 80–126.
- Baken, E. K., Collyer, M. L., Kaliontzopoulou, A., & Adams, D. C. (2021). geomorph v4.0 and gmShiny: Enhanced analytics and a new graphical interface for a comprehensive morphometric experience. *Methods in Ecology and Evolution*, 12, 2355–2363.
- Bell, P. R., Snively, E., & Shychoski, L. (2009). A comparison of the jaw mechanics in hadrosaurid and ceratopsid dinosaurs using finite element analysis. *The Anatomical Record: Advances in Integrative Anatomy and Evolutionary Biology*, 292, 1338–1351.
- Brink, K. S., Zelenitsky, D. K., Evans, D. C., Therrien, F., & Horner, J. R. (2011). A sub-adult skull of *Hypacrosaurus stebingeri* (Ornithischia: Lambeosaurinae): Anatomy and comparison. *Historical Biology*, 23(1), 63–72.
- Brusatte, S. L., Sakamoto, M., Montanari, S., & Harcourt Smith, W. E. H. (2011). The evolution of cranial form and function in theropod dinosaurs: Insights from geometric morphometrics. *Journal of Evolutionary Biology*, 25, 365–377.
- Byron, C., Segreti, M., Hawkinson, K., Herman, K., & Patel, S. (2018). Dietary material properties shape cranial suture morphology in the mouse calvarium. *Journal of Anatomy*, 233, 807–813.
- Carrano, M. T., Janis, J. M., & Sepkoski, J. J., Jr. (1999). Hadrosaurs as ungulate parallels: Lost lifestyles and deficient data. *Acta Palaeontologica Polonica*, 44(3), 237–261.

- Chapman, R. E., & Brett-Surman, M. K. (1990). Morphometric observations on hadrosaurid ornithopods. In K. Carpenter, & P. J. Currie (Eds.), *Dinosaur systematics: Approaches and perspectives* (pp. 163–177). Cambridge University Press.
- Dodson, P. (1975). Taxonomic implications of relative growth in Lambeosaurine Hadrosaurs. *Systematic Zoology*, 24, 37–54.
- Enlow, D. H. (1989). Normal and abnormal patterns of craniofacial growth. In J. A. Persing, M. T. Edgerton, & J. A. Jane (Eds.), *Scientific foundations and surgical treatment of craniosynostosis* (pp. 83–86). Williams & Wilkins.
- Erickson, G. M., Krick, B. A., Hamilton, M., Bourne, G. R., Norell, M. A., Lilleodden, E., & Sawyer, W. G. (2012). Complex dental structure and wear biomechanics in hadrosaurid dinosaurs. *Science*, 338, 98–101.
- Evans, D. C. (2010). Cranial anatomy and systematics of *Hypacrosaurus altispinus*, and a comparative analysis of skull growth in Lambeosaurine hadrosaurids (Dinosauria: Ornithischia): Cranial anatomy of *Hypacrosaurus altispinus*. *Zoological Journal of the Linnean Society*, 159, 398–434.
- Evans, D. C., Forster, C. A., & Reisz, R. R. (2005). The type specimen of *Tetragonosaurus erectofrons* (Ornithischia: Hadrosauridae), and the taxonomic identity of juvenile lambeosaurines from the Dinosaur Park Formation, Alberta, Canada. In P. J. Currie, & E. Koppelhus (Eds.), *Dinosaur Provincial Park*. Indiana University Press.
- Evans, D. C., Reisz, R. R., & Dupuis, K. (2007). A juvenile *Parasaurolophus* (Ornithischia: Hadrosauridae) braincase from Dinosaur Provincial Park, Alberta, with comments on crest ontogeny in the genus. *Journal of Vertebrate Paleontology*, 27(3), 642–650.
- Felice, R. N., Watanabe, A., Cuff, A. R., Hanson, M., Bhullar, B.-A. S., Rayfield, E. R., Witmer, L. M., Norell, M. A., & Goswami, A. (2020). Decelerated dinosaur skull evolution with the origin of birds. *PLoS Biology*, 18(8), e3000801.
- Fortuny, J., Marcé-Nogué, J., Heiss, E., Sanchez, M., Gil, L., & Galobart, À. (2015). 3D bite modeling and feeding mechanics of the largest living amphibian, the Chinese giant salamander *Andrias davidianus* (Amphibia: Urodela). *PLoS ONE*, 10(4), e0121885.
- Foth, C., Hedrick, B. P., & Ezcurra, M. D. (2016). Cranial ontogenetic variation in early saurischians and the role of heterochrony in the diversification of predatory dinosaurs. *PeerJ*, 4, e1589.
- Gruntmejer, K., Konietzko-Meier, D., Bodzioch, A., & Fortuny, J. (2019). Morphology and preliminary biomechanical interpretation of mandibular sutures in *Metoposaurus krasiejowensis* (Temnospondyli, Stereospondyli) from the Upper Triassic of Poland. *Journal of Iberian Geology*, 45, 301–316.
- Herring, S. W. (1972). Sutures—a tool in functional cranial analysis. *Cells Tissues Organs*, 83, 222–247.
- Herring, S. W. (1993). Formation of the vertebrate face: Epigenetic and functional influences. *American Zoologist*, 33, 472–483.
- Herring, S. W. (2008). Mechanical influences on suture development and patency. *Frontiers in Oral Biology*, 12, 41–56.
- Herring, S. W., & Mucci, R. J. (1991). In vivo strain in cranial sutures: The zygomatic arch. *Journal of Morphology*, 207, 225–239.
- Herring, S. W., & Teng, S. (2000). Strain in the braincase and its sutures during function. *American Journal of Physical Anthropology*, 112, 575–593.
- Hopson, J. A. (1975). The evolution of cranial display structures in hadrosaurian dinosaurs. *Paleobiology*, 1(1), 21–43.
- Jaslow, C. R. (1989). Sexual dimorphism of cranial suture complexity in wild sheep (*Ovis orientalis*). *Zoological Journal of the Linnean Society*, 95(4), 273–284.
- Jaslow, C. R. (1990). Mechanical properties of cranial sutures. *Journal of Biomechanics*, 23(4), 313–321.
- Kammerer, C. F. (2021). Elevated cranial sutural complexity in burrowing dicynodonts. *Frontiers in Ecology and Evolution*, 9, 674151.
- Katze, W. (1999). Comparative morphology and functional interpretation of the sutures in the dermal skull roof of temnospondyl amphibians. *Zoological Journal of the Linnean Society*, 126, 1–39.
- Lowi-Merri, T. M., & Evans, D. C. (2020). Cranial variation in *Gryposaurus* and biostratigraphy of hadrosaurines (Ornithischia: Hadrosauridae) from the Dinosaur Park Formation of Alberta, Canada. *Canadian Journal of Earth Sciences*, 57, 765–779.
- Mallon, J. C. (2019). Competition structured a Late Cretaceous megaherbivorous dinosaur assemblage. *Scientific Reports*, 9, 15447.
- Mallon, J. C., & Anderson, J. S. (2013). Skull ecomorphology of megaherbivorous dinosaurs from the Dinosaur Park Formation (upper Campanian) of Alberta, Canada. *PLoS ONE*, 8(7), e67182.
- Mallon, J. C., & Anderson, J. S. (2015). Jaw mechanics and evolutionary paleoecology of the megaherbivorous dinosaurs from the Dinosaur Park Formation (upper Campanian) of Alberta, Canada. *Journal of Vertebrate Paleontology*, 35(2), e904323.
- Mallon, J. C., Evans, D. C., Zhang, Y., & Xing, H. (2022). Rare juvenile material constrains estimation of skeletal allometry in *Gryposaurus notabilis* (Dinosauria: Hadrosauridae). *The Anatomical Record*, 1–23.
- Maloul, A., Fialkov, J., Wagner, D., & Whyne, C. M. (2014). Characterization of craniofacial sutures using the finite element method. *Journal of Biomechanics*, 47(1), 245–252.
- Markey, M. J., & Marshall, C. R. (2007). Linking form and function of the fibrous joints in the skull: A new quantification scheme for cranial sutures using the extant fish *Polypterus endlicherii*. *Journal of Morphology*, 268, 89–102.
- Meyer, D., Dimitriadou, E., Hornik, E., Weingessel, A., & Leisch, F. (2021). *e1071: Misc functions of the department of statistics, Probability Theory Group (Formerly: E1071), TU Wien. R package version 1. 7–9*. <https://cran.r-project.org/web/packages/e1071/index.html>
- Monteiro, L. R., & Lessa, L. G. (2000). Comparative analysis of cranial suture complexity in the genus *Caiman* (Crocodylia, Alligatoridae). *Revista Brasileira de Biologia*, 60(4), 689–694.
- Moss, M. L. (1954). Growth of the calvaria in the rat. The determination of osseous morphology. *American Journal of Anatomy*, 94, 333–361.
- Moss, M. L. (1957). Experimental alteration of sutural area morphology. *The Anatomical Record*, 127, 569–589.
- Moss, M. L. (1961). Extrinsic determination of sutural area morphology in the rat calvaria. *Cells Tissues Organs*, 44, 263–272.

- Nabavizadeh, A. (2016). Evolutionary trends in the jaw adductor mechanics of ornithischian dinosaurs. *The Anatomical Record*, 299, 271–294.
- Olsen, A. M., & Westneat, M. W. (2015). StereoMorph: an R package for the collection of 3D landmarks and curves using a stereo camera set-up. *Methods in Ecology and Evolution*, 6(3), 351–356.
- Porro, L. B., Rayfield, E. J., & Clack, J. A. (2015). Descriptive anatomy and three-dimensional reconstruction of the skull of the early tetrapod *Acanthostega gunnari* Jarvik, 1952. *PLoS ONE*, 10(3), e0118882.
- Prieto-Márquez, A. (2010). Global phylogeny of Hadrosauridae (Dinosauria: Ornithopoda) using parsimony and Bayesian methods: Phylogeny of Hadrosaurid dinosaurs. *Zoological Journal of the Linnean Society*, 159, 435–502.
- R Core Team. (2021). *R: A language and environment for statistical computing*. R Foundation for Statistical Computing.
- Rafferty, K. L., & Herring, S. W. (1999). Craniofacial sutures: Morphology, growth, and in vivo masticatory strains. *Journal of Morphology*, 242(2), 167–179.
- Rayfield, E. J. (2004). Cranial mechanics and feeding in *Tyrannosaurus rex*. *Proceedings for the Royal Society of London B*, 271, 1451–1459.
- Rayfield, E. J. (2005). Using finite-element analysis to investigate suture morphology: A case study using large carnivorous dinosaurs. *The Anatomical Record Part A: Discoveries in Molecular, Cellular, and Evolutionary Biology*, 283A, 349–365.
- Rybczynski, R., Tirabasso, A., Bloskie, P., Cuthbertson, R., & Holliday, C. (2008). A three-dimensional animation model of *Edmontosaurus* (Hadrosauridae) for testing chewing hypotheses. *Palaeontologia Electronica*, 11(2), 9A.
- Savoldi, F., Tsoi, J. K. H., Paganelli, C., & Matinlinna, J. P. (2019). Sutural morphology in the craniofacial skeleton: A descriptive microcomputed tomography study in a swine model. *The Anatomical Record*, 302(12), 2156–2163.
- Schneider, C. A., Rasband, W. S., & Eliceiri, K. W. (2012). NIH Image to ImageJ: 25 years of image analysis. *Nature Methods*, 9, 671–675.
- Sereno, P. C. (1998). A rationale for phylogenetic definitions, with application to the higher-level taxonomy of Dinosauria. *Neues Jahrbuch für Geologie und Paläontologie - Abhandlungen*, 210, 41–83.
- Sereno, P. C. (2005, September 17). *Stem Archosauria version 1.0*. TaxonSearch. <http://www.taxonsearch.org/Archive/stemarchosauria-1.0.php>
- Stoica, P., & Moses, R. (1997). *Introduction to spectral analysis*. Prentice-Hall.
- Weishampel, D. B. (1984). Evolution of jaw mechanisms in ornithopod dinosaurs. *Advances in Anatomy, Embryology and Cell Biology*, 87, 1–10.
- White, H. E., Clavel, J., Tucker, A. S., & Goswami, A. (2020). A comparison of metrics for quantifying cranial suture complexity. *Journal of the Royal Society Interface*, 17(171), 20200476.
- White, H. E., Goswami, A., & Tucker, A. S. (2021). The intertwined evolution and development of sutures and cranial morphology. *Frontiers in Cell and Developmental Biology*, 9, 653579.
- Xing, L., Niu, K., Yang, T.-R., Wang, D., Miyashita, T., & Mallon, J. C. (2022). Hadrosauroid eggs and embryos from the Upper Cretaceous (Maastrichtian) of Jiangxi Province, China. *BMC Ecology and Evolution*, 22, 60.

SUPPORTING INFORMATION

Additional supporting information can be found online in the Supporting Information section at the end of this article.

How to cite this article: Dudgeon, T. W., & Evans, D. C. (2023). Calvarial suture interdigitation in hadrosaurids (Ornithischia: Ornithopoda): Perspectives through ontogeny and evolution. *Evolution & Development*, 1–17. <https://doi.org/10.1111/ede.12430>